


Wide spectral coverage (0.7–2.2 eV) lattice-matched multijunction solar cells based on AlGaInP, AlGaAs and GaInNAsSb materials

Arto Aho  | Riku Isoaho  | Marianna Raappana  | Timo Aho  |
Elina Anttola | Jari Lyytikäinen | Arttu Hietalahti | Ville Polojärvi  |
Antti Tukiainen  | Jarno Reuna  | Leo Peltomaa | Mircea Guina 

Optoelectronics Research Centre, Physics Unit, Tampere University, Tampere, Finland

Correspondence

Arto Aho, Optoelectronics Research Centre, Physics Unit, Tampere University, Tampere, Finland.

Email: arto.aho@tuni.fi

Funding information

Academy of Finland, Grant/Award Number: PREIN #320168; H2020 European Research Council, Grant/Award Number: ERC-2015-AdG 695116

Abstract

We report on the progress in developing lattice-matched GaAs-based solar cells with focus on developing AlGaInP, AlGaAs, and GaInNAsSb materials, aiming at achieving a wide spectral coverage, that is, 0.7–2.2 eV. To this end, we first benchmark the performance of an upright four-junction GaInP/GaAs/GaInNAsSb/GaInNAsSb solar cells grown by molecular beam epitaxy on p-GaAs substrates with bandgaps of 1.88, 1.42, 1.17, and 0.93 eV, respectively. The four-junction cell exhibited an efficiency of ~39% at 560-sun illumination while showing good electrical performance even up to 1000 suns. As a first step to further improve the efficiency toward 50% level, we demonstrate AlGaInP (>2 eV) and GaInNAsSb (<0.8 eV) subcells. We prove that AlGaInP cells with 0.1 Al composition would exhibit current-matching condition when being incorporated in a five-junction architecture together with two GaInNAsSb bottom and AlGaAs top junctions. Furthermore, current matching required for a six-junction tandem architecture is achieved for an Al composition of 0.26. Overall, the results open a practical path toward fabrication of lattice-matched solar cells with more than four junctions.

KEYWORDS

AlGaInP, dilute nitrides, molecular beam epitaxy, multijunction solar cells

1 | INTRODUCTION

III–V semiconductor materials are commonly used for fabricating the most efficient multijunction solar cells, with record efficiency set to 47.1% for an architecture with six monolithic junctions fabricated with an inverted metamorphic process.¹ Metamorphic approaches usually require growth of thick buffer layers between junctions that have different lattice constants. Ideally, the entire multijunction solar cell structure would be monolithically grown and would have the same lattice constant for all the junctions. In theory, such lattice-matched

(LM) III–V solar cell with more than four junctions (4J) can achieve efficiencies of over 50% under concentrated sunlight, that is, concentrated photovoltaics (CPV) operation, and over 35% for space operation. It would also be beneficial to fabricate the structure in an upright architecture, which simplifies the epi-wafer processing, increases the yield, and requires handling of only one wafer. Upright III–V triple-junction (3J) solar cells have been fabricated for more than a decade,^{2–4} and recently, also 4J solar cells have been reported with metamorphic² and LM approaches.^{5–8} The upright LM approach is particularly interesting, because besides the fact that it avoids the use

This is an open access article under the terms of the Creative Commons Attribution License, which permits use, distribution and reproduction in any medium, provided the original work is properly cited.

© 2021 The Authors. Progress in Photovoltaics: Research and Applications published by John Wiley & Sons Ltd.

of metamorphic buffer layers, it can make use of the same tunnel junctions that have been long time optimized for the LM 3J solar cells. Moreover, the LM approach is the most efficient strategy in terms of material utilization given their reduced thickness, a feature that becomes more evident for architectures with four or more subcells.

One of the essential steps in developing the LM multijunction approach has been the progress in epitaxy of GaInNAsSb junction materials with bandgap covering the 0.8–1 eV spectral range. To this end, an upright LM 4J GaInP/GaAs/GaInNAsSb/GaInNAsSb solar cell monolithically grown on GaAs by molecular beam epitaxy (MBE) was reported recently.⁸ This first demonstration of 4J design including two dilute nitride subcells, which is schematically shown in Figure 1, exhibited an efficiency of 25% at one-sun illumination, whereas an efficiency of 37% was already demonstrated under 100-sun illumination. It was also estimated that efficiency of 47% seems feasible under higher concentration for an optimized design.

In this paper, we present the progress in developing 4J LM solar cell outlining the need to further extend the spectral coverage toward 0.7 eV at the long wavelengths and beyond 2 eV for the short wavelengths. To this end, we present the development of narrow bandgap (~ 0.7 eV) GaInNAsSb junctions and of AlGaInP high-bandgap (>2 eV) junctions, enabling a more efficient conversion in a wider spectral range. Additional developments toward achieving the 50% efficiency target are also discussed.

2 | EXPERIMENTS

Epitaxial solar cell structures were grown upright on p-GaAs substrates using Veeco GEN20 and VG Semicon V90 MBE systems.

Detailed description for the MBE processes related to GaInNAsSb fabrication are given elsewhere.^{9–11} First, a 4J LM GaInP/GaAs/GaInNAsSb/GaInNAsSb solar cell with subjunction bandgaps of 1.88, 1.42, 1.17, and 0.93 eV was fabricated. This development was done in parallel with optimization of the lowest/highest bandgap heterostructures discussed in the paper with the purpose of revealing the current level of technology progress for the 4J LM solar cells and point the direction of developments toward increasing the number of junctions. For assessing the photovoltaic properties of high-bandgap materials required in architecture with more than 4J, we grow single-junction $(\text{Al}_x\text{Ga}_{1-x})_{1-y}\text{In}_y\text{P}$ solar cells with the Al composition x ranging from 0 to 0.6, corresponding to bandgaps of 1.9–2.2 eV. The In composition y was set to ~ 0.48 to ensure lattice matching to GaAs. Moreover, single-junction solar cells with bandgaps between 1.4 and 1.9 eV were fabricated using $\text{Al}_x\text{Ga}_{1-x}\text{As}$ by varying the Al composition from 0 to 0.4. Finally, the full spectrum coverage required for architectures with more than 4J was achieved by growing GaInNAsSb single-junction cells with varying In, N, and Sb compositions and a balance of $[\text{In}] = 2.7 \times [\text{N}]$ and $[\text{Sb}] = 2.4 \times [\text{N}]$.¹² In this case, we aimed at ensuring lattice matching to GaAs and bandgap variation ranging from 1.4 down to 0.7 eV. For some of the subjunctions, also isotype single-junction cells were fabricated, with passive semiconductor layers on top to mimic the optical losses of the top junctions. These solar cells were needed for more accurate subjunction performance estimation, as well as for calibration of the OAI solar simulator for the 4J solar cell measurements. The solar cells were processed by forming Au-based contacts on both sides of the chips. A $\text{TiO}_x/\text{SiO}_y$ antireflection coating was deposited by e-beam evaporation on the front side of most of the solar cells reported. The dilute nitride junctions are p-i-n

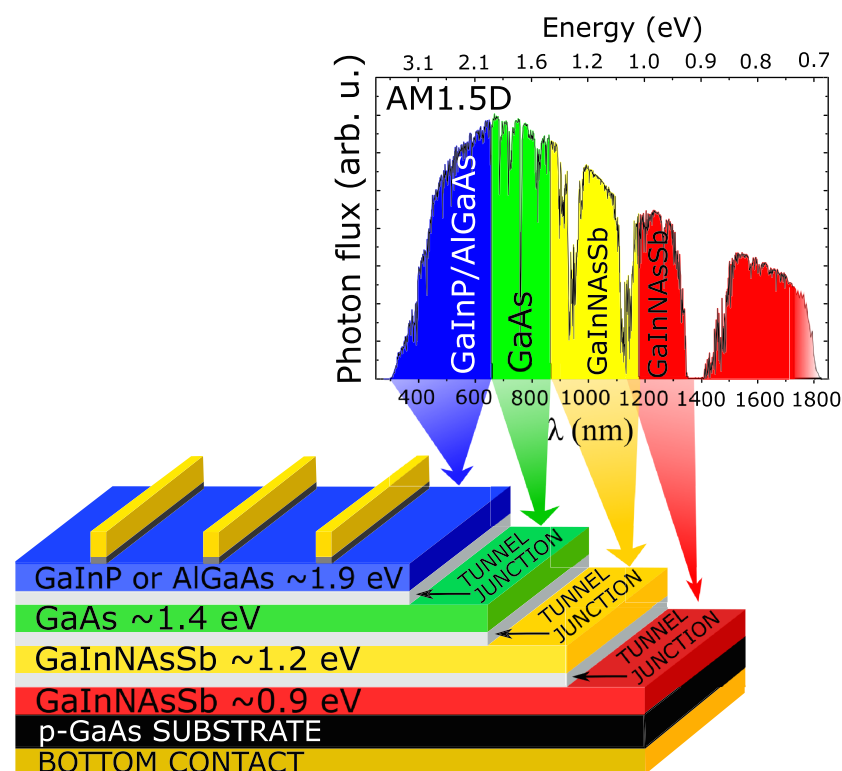


FIGURE 1 Schematic structure of the LM 4J solar cell [Colour figure can be viewed at wileyonlinelibrary.com]

structures, and all other junctions are shallow emitter n-on-p structures. The tunnel junctions are AlGaAs/GaAs heterostructures.

The current–voltage (IV) characteristics of all cells were measured at 1 sun. In addition, the LM 4J solar cell was measured with concentration up to 1000 suns. These measurements were performed using a commercial steady-state OAI 7-kW TriSOL solar simulator. External quantum efficiency (EQE) measurements were performed using an in-house built system for measuring single- and multijunction solar cells. In addition, the internal quantum efficiencies (IQE) for AlGaInP solar cells were estimated using EQE and reflectance data. The short-circuit current densities (J_{sc}) of the AlGaInP single-junction solar cells and LM 4J subjunctions were estimated from EQE and IQE data. ASTM G173-3 AM1.5D (1000 W/m²) spectrum was used as the reference spectrum. The performance of the LM 4J solar cell was modeled using simple diode equations that have been earlier validated for dilute nitride-based 3J and 4J solar cells.⁸

3 | RESULTS AND DISCUSSION

The EQE results of the best LM 4J is presented in Figure 2. As it can be seen, this structure covers efficiently the spectral range of 350–1310 nm, in which intra-band efficiency can theoretically reach over 52% efficiency under 1000-sun illumination.⁸ Compared with earlier results, we note that the three topmost junctions have been thinned to achieve close to current-matching condition. The three topmost optically thin junctions have thicknesses of 400, 600, and 1000 nm, respectively. For this particular cell, the estimated J_{sc} values for different subjunctions under AM1.5D (1000 W/cm²) illumination

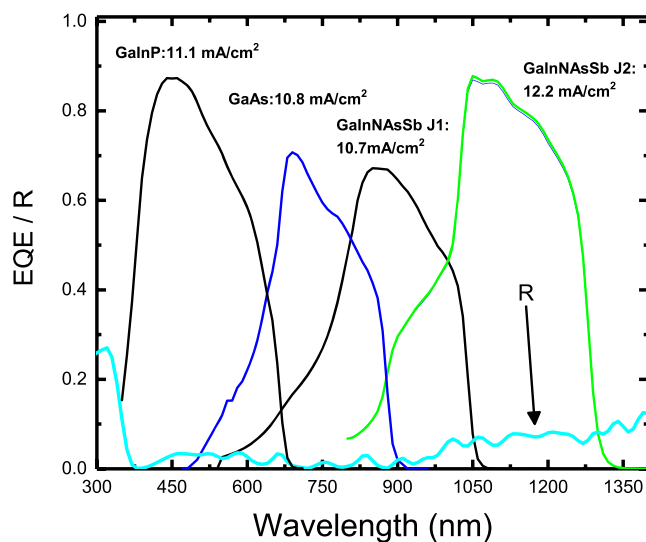


FIGURE 2 EQE data for an improved LM 4J. The responses of different subjunction overlaps, which require careful selection and control of the light biasing. The graph also shows the surface reflectivity (R). The sharp cutoff at 800 nm for the bottom junction EQE is due to the optical filter implemented in our EQE system (800-nm high-pass filter) [Colour figure can be viewed at wileyonlinelibrary.com]

are 11.1, 10.8, 10.7, and 12.2 mA/cm² for GaInP, GaAs, GaInNASb (1.17 eV), and GaInNASb (0.93 eV), respectively. Assuming the use of materials with optimal bandgaps of 2.0, 1.51, 1.16, and 0.79 eV, we estimate to be plausible achieving an efficiency of 49.8% at 1500 suns, owing to reduced transmission and thermalization losses. To this end, we will later discuss the results obtained in developing high-bandgap >1.9-eV AlGaInP and low-bandgap <0.9-eV GaInNASb materials.

The IV characteristics of the LM 4J solar cell are shown in Figure 3. An open-circuit voltage (V_{oc}) of 3.24 V was achieved for a 2 × 2 mm component and 3.27 V for a 5 × 5 mm component (IV curve is not shown here). The two dilute nitride junctions in the LM 4J provide a voltage of nearly 1 V. It is assumed that the small difference between the V_{oc} values originates from the different perimeter-to-area ratios, leading to different recombination rates at the facets,¹³ yet the V_{oc} value is significantly higher than what was exhibited for the first demonstration (2.94 V).⁸ Theoretically, we estimate that the LM 4J could exhibit a V_{oc} of 3.38 V, of which 97% has been now achieved. Moreover, the LM 4J cell exhibited a bandgap voltage offset of 0.53 V per junction and fill factor (FF) value of 82%. The 1-sun efficiency value was 29%, whereas a value of 32% was estimated for a perfectly current-matched design. Moreover, Figure 3 shows the diode model of the IV characteristics at 1 sun using the J_{sc} values calculated from the EQE data, revealing an excellent fit to the experimental curve. For the 1-sun setup of our solar simulator, we estimate that the biasing conditions are following: 1.00, 0.88, 0.98, and 1.03 for GaInP, GaAs, GaInNASb (1.2 eV), and GaInNASb (0.95 eV), respectively. These values were calibrated using isotype solar cells that correspond to the subjunctions of the measured 4J. The 1-sun evaluation of the 4J in these conditions gives measurement that is limited by the second junction. The misfit values are calculated

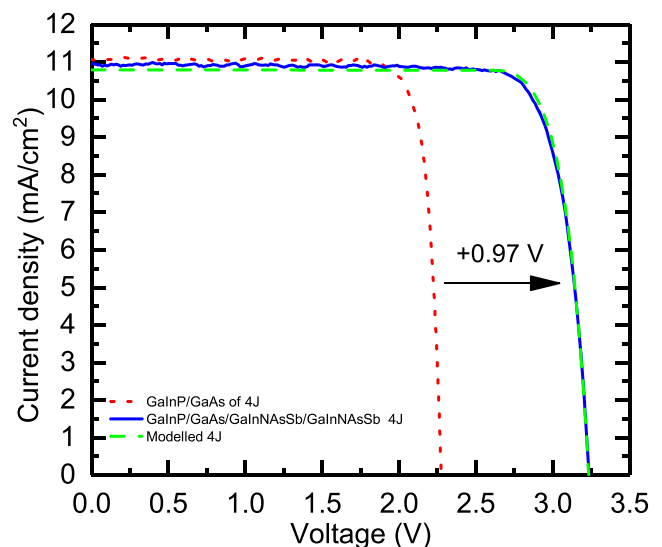


FIGURE 3 One-sun IV characteristics of LM 4J and modeled IV performance. The IV curve of a GaInP/GaAs 2J tandem used in the 4J stack is also shown [Colour figure can be viewed at wileyonlinelibrary.com]

by dividing the measured subcell J_{sc} by the calculated J_{sc} value of the subcell (derived by EQE) and divided by the top junction J_{sc} value of the corresponding conditions.

The CPV performance of the cell is summarized in Table 1 and shown in Figure 4 using a CPV solar simulator. The results show that the improved LM 4J of this work has significantly lower resistive losses than the LM 4J demonstrated in ref.⁸, which in turn helps to achieve higher FF values and an efficiency of about 39%. In addition, the V_{oc} is over 4.1 V, and the cell maintains high efficiency even close to 1000 suns. These improvements are attributed to better charge carrier transport properties of the top GaInP solar cell compared to the top AlGaAs solar cell used in ref.⁸. The front grid pattern was also modified, and the size of solar cell device was increased from 1×1 to 2×2 mm. We want to note here that the simulator is target spectrum is AM1.5D, but when the measured subjunction J_{sc} values are compared to the corresponding EQE-calibrated J_{sc} values, we find the following bias nonidealities (misfits). The top cell current is well calibrated and matches the EQE data, but the second, third, and fourth subjunctions are overbiased to 1.093, 1.095, and 1.269 times, respectively, when compared with the photocurrent generation determined from EQE. These numbers show that the 4J solar cell could not be measured using exact subcell biasing, which resulted in top SC-limited measurement, even though when matched to the AM1.5D standard the third cell should limit. For more accurate efficiency determination, the solar cell should be measured under certified CPV conditions. Based on a separate spectrally dynamic analysis (not included here), we estimate that FF might be underestimated by 2–3 percentage points due to the bias mismatch and spectral impurity. We note that when the intensity of CPV simulator is reduced to close to 1 sun while maintaining the spectrum, the FF is only 81%, which is actually lower than what we get when the 1-sun setup is used for the OAI simulator. This points that under high intensities, the FF values are slightly underestimated when the CPV setup is used. We estimate that the reason for the difference in FF at 1 sun originate from difference in the blue end intensity, which is lower for CPV measurement mode. Further investigations will be conducted to confirm the exact FF values at high intensities. We estimate that the current over-generation in the fourth cell does not play a significant role for

TABLE 1 Temperature-corrected efficiency values for the LM 4J cell under CPV operation

Intensity (suns)	FF (%)	V_{oc} (V)	Efficiency (%)
1	81.9	3.24	29.6
110	82.1	3.96	37.0
564	82.6	4.13	39.3
946	80.4	4.17	36.9

Note: The temperature-corrected values were calibrated using externally verified reference solar cells (Azur Space 3J CPV solar cells). In addition, the temperature coefficients were measured at different intensities (not shown here).

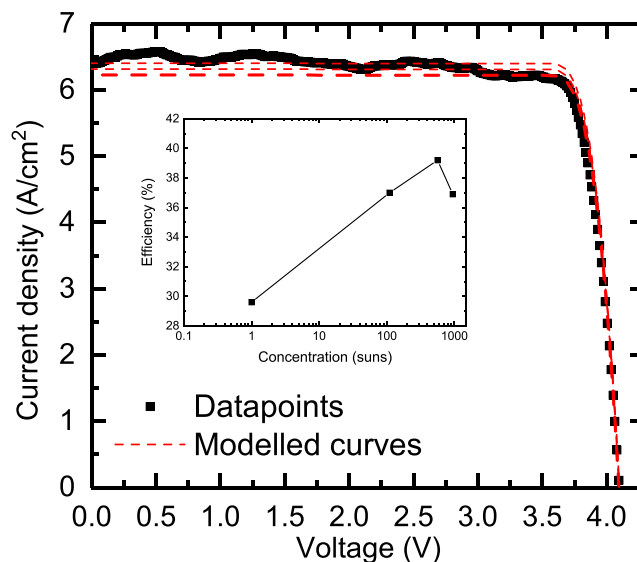


FIGURE 4 IV characteristics of LM 4J at over 500 suns. The inset shows the trend of efficiency versus light concentration. A good fit can be seen between the modeled IV characteristics and the experimental data. For the modeled curves in red, the J_{sc} values have slight offset for differentiation [Colour figure can be viewed at wileyonlinelibrary.com]

assessing the 4J performance, because it was not limiting or even close to be the limiting subjunction. The values in the table are temperature corrected using separately determined reference data. We want to emphasize that even though the spectrum used for the 4J performance evaluation is not pure enough for efficiency verification, the results show that the FF is not severely limited by resistive losses up to 946 suns. This shows that after fine-tuning, these SCs could be used realistically in high CPV systems.

The LM 4J performance could be improved by further reducing the reflectance of the antireflection coating that has an average value of 3%. Moreover, the collection losses of the junctions are estimated to amount for about 8% and are caused mainly by the transmission losses of the bottom junction. The J_{sc} distribution of the LM 4J solar cell is graphically illustrated in Figure 5. We note that the estimated absorption losses in the top tunnel junction are only 1%.

Next, we focus on presenting the main results obtained for the high-bandgap and low-bandgap heterostructures required in architectures with more than 4J. It is generally accepted that growing high-performance AlGaInP solar cells, LEDs, and lasers is challenging independent of the growth method. Typically, the more there is Al in AlGaInP, the more severe the challenges are. Nonoptimal material characteristics have been caused, for instance, by oxygen and boron impurities,^{14–16} partly originating from the reactive nature of Al and strong bonds of Al compounds. In addition, issues with doping activation and low charge carrier mobilities can increase the resistive losses and cause low charge collection efficiencies. These limitations have been also reflected in our study that reported the EQE response of the AlGaInP solar cells and shown in Figure 6; it can be seen that for Al compositions ≥ 0.5 , the EQE response is significantly reduced. The

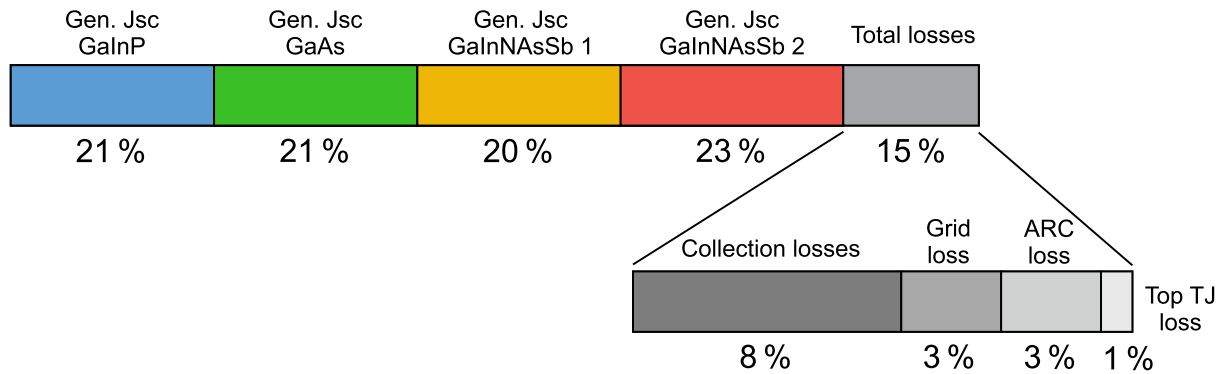


FIGURE 5 J_{sc} spectral distribution for different subcells of the LM 4J solar cell (AM1.5D spectrum) [Colour figure can be viewed at wileyonlinelibrary.com]

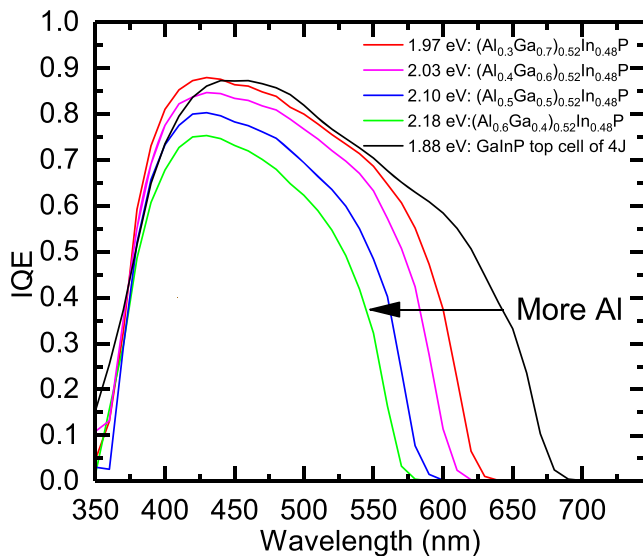


FIGURE 6 Measured IQE values for AlGaInP solar cells grown with 0–0.6 Al composition [Colour figure can be viewed at wileyonlinelibrary.com]

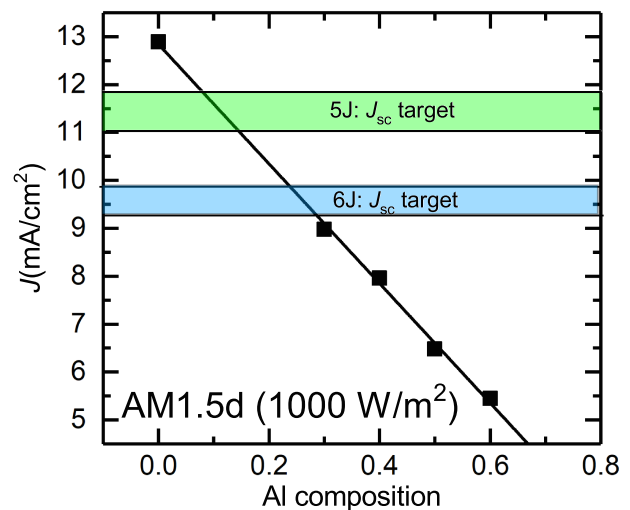


FIGURE 7 Calculated J_{sc} values for MBE-grown AlGaInP solar cells as the function of Al composition. The input spectrum ASTM G173-3 AM1.5D (1000 W/m²) was used [Colour figure can be viewed at wileyonlinelibrary.com]

AlGaInP solar cells could in principle generate a high enough current to be utilized in five- (5J) and six-junction (6J) solar cells, but when compared to GaInP, special attention needs to be given to the increased series resistance, which in practice still limits the performance of AlGaInP solar cells of this study. The calculated J_{sc} values for AlGaInP solar cells are presented in Figure 7. In the same figure, the required J_{sc} values for 5J and 6J solar cells incorporating a high-performance 0.7-eV bottom junction are illustrated. Based on these results, Al compositions of 0.10 and 0.26 could be used for the AlGaInP top cell in current-matched 5J and 6J structures, respectively (see Figure 7). More detailed studies are needed to further reduce the series resistance of the AlGaInP subjunction that enables high CPV operation.

When it comes to lowest bandgap component, it has been challenging to fabricate GaInNAsSb compounds with high N composition. In high-performance multijunction solar cells, the bandgap of the GaInNAsSb junction has been typically limited to energies higher than 0.9 eV. Recently, we have demonstrated that high-performance

narrow-bandgap (<0.8 eV) junctions can have good current generation¹⁰ and have potential to be usable as bottom junctions for 5J and 6J architectures. For the dilute nitride solar cells, the series resistance is clearly not an issue, but maintaining high charge carrier lifetimes and low background doping levels is even more critical for high (>6%) N content. As seen in Figure 8, the state-of-the-art narrow-bandgap GaInNAsSb solar cells have almost as high spectral response as the typical Ge junctions. If collection efficiency of GaInNAsSb i-region can be improved for the 0.73-eV solar cell, the higher absorption of direct bandgap GaInNAsSb could potentially harvest even more photons than the indirect bandgap Ge junctions.

Finally, Figure 9 illustrates also the 1-sun V_{oc} values for single-junction solar cells with different bandgaps. The results show that the more Al in AlGaInP or the more N in GaInNAsSb is used, the more challenging it is to maintain high V_{oc} values. Despite these challenges, it can be stated that the full spectrum coverage is plausible using MBE processes on GaAs substrates and that the structure can be rather freely and simply optimized for minimizing the transmission and thermalization losses. Calculations predict that when these materials are

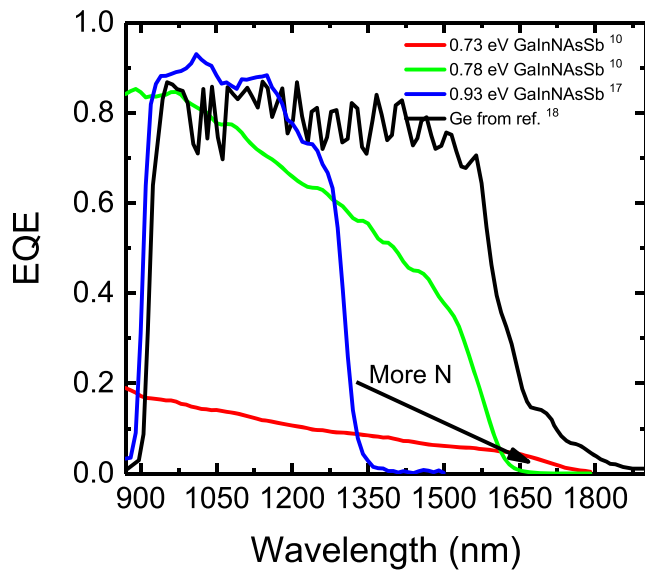


FIGURE 8 EQE measurements of narrow-bandgap GaInNAsSb solar cells and reference Ge EQE curve from ref.¹⁷ [Colour figure can be viewed at wileyonlinelibrary.com]

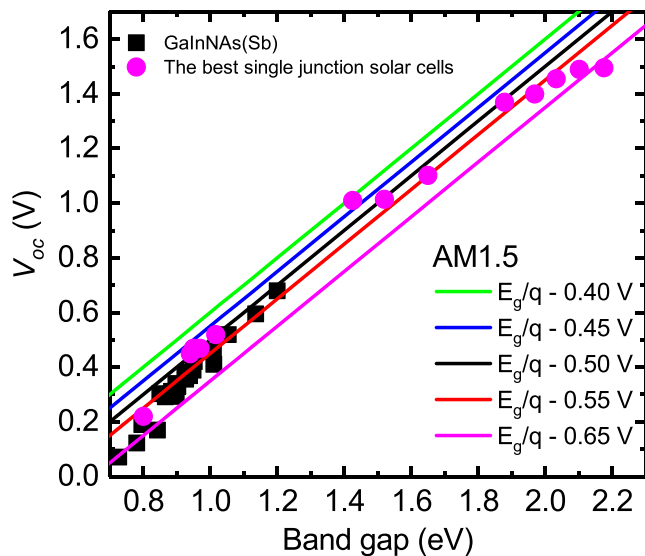


FIGURE 9 V_{oc} values for MBE-grown LM single-junction solar cells demonstrated by the authors [Colour figure can be viewed at wileyonlinelibrary.com]

integrated within an optimal LM 6J structure, over 50% efficiencies could be expected under concentrated sunlight.¹⁰

4 | CONCLUSIONS

A state-of-the-art 4J upright LM GaInP/GaAs/GalnNAsSb/GalnNAsSb solar cells grown by MBE on p-GaAs substrates is demonstrated. The corresponding bandgaps are 1.88, 1.42, 1.17, and 0.93 eV. The 4J solar cell exhibited an efficiency of 39% at 560-sun illumination while showing good electrical performance even up to

1000 suns with V_{oc} of over 4.1 V. Moreover, we demonstrate high spectral response for AlGaInP junctions with bandgap of 2.2 eV and GaInNAsSb with bandgap of 0.73 eV, which are instrumental for advancing the tandem architecture to include more than 4J. In particular, we prove that AlGaInP with Al compositions of 0.1 and 0.26 would satisfy current-matching condition when a 0.7-eV bottom cell would be incorporated to 5J and 6J solar cells, respectively.

ACKNOWLEDGEMENTS

The authors acknowledge the H2020 European Research Council AdG project AMETIST (Grant Agreement No. ERC-2015-AdG 695116) for financing the study. This work is part of the Academy of Finland Flagship Programme PREIN #320168.

ORCID

Arto Aho <https://orcid.org/0000-0003-2744-929X>

Riku Isoaho <https://orcid.org/0000-0002-0582-3853>

Marianna Raappana <https://orcid.org/0000-0003-1034-5523>

Timo Aho <https://orcid.org/0000-0001-5020-1415>

Ville Polojärvi <https://orcid.org/0000-0001-9490-0672>

Antti Tukiainen <https://orcid.org/0000-0003-2227-833X>

Jarno Reuna <https://orcid.org/0000-0003-0814-1740>

Mircea Guina <https://orcid.org/0000-0002-9317-8187>

REFERENCES

- Geisz JF, France RM, Schulte KL, et al. Six-junction III-V solar cells with 47.1% conversion efficiency under 143 suns concentration. *Nat Energy*. 2020;5(4):326-335.
- Guter W, Dunzer F, Ebel L, et al. Space solar cells – 3G30 and next generation radiation hard products. *E3S Web Conf*. 2017;16:1-6. <https://doi.org/10.1051/e3sconf/20171603005>
- Green MA, Emery K, Hishikawa Y, Warta W, Dunlop ED. Solar cell efficiency tables (version 41). *Prog Photovolt: Res Appl*. 2013;21(1):1-11.
- Aho A, Isoaho R, Tukiainen A, et al. Temperature coefficients for GaInP/GaAs/GalnNAsSb solar cells. *AIP Conference Proceedings*. 2015;1679(1):1-5.
- King RR, Colter PC, Joslin DE, et al. High-voltage, low-current GaInP/GaAs/GalnNAsSb solar cells. *29th IEEE Photovoltaic Specialists Conference*. 2002;852-855. <https://doi.org/10.1109/PVSC.2002.1190713>
- Essig S, Stammler E, Rönsch S, et al. Dilute Nitrides for 4- and 6-Junction Space Solar Cells. *9th European Space Power Conference 2011. Proceedings. CD-ROM: 6-10 June 2011, Saint Raphael, France. Noordwijk: ESA, 2011. (ESA SP 690)*. European Space Agency; 2011.
- Ochoa M, García I, Lombardero I, et al. Modelling of lattice matched dilute nitride 4-junction concentrator solar cells on Ge substrates. *AIP Conference Proceedings*. 2016;1766:1-7. <https://doi.org/10.1063/1.4962101>
- Aho A, Isoaho R, Hytönen L, et al. Lattice-matched four-junction tandem solar cell including two dilute nitride bottom junctions. *Prog Photovolt Res Appl*. 2018;27:299-305.
- Aho A, Polojärvi V, Korpjärvi V-M, et al. Composition dependent growth dynamics in molecular beam epitaxy of GaInNAs solar cells. *Solar Energy Materials and Solar Cells*. 2014;124:150-158.
- Isoaho R, Aho A, Tukiainen A, et al. Photovoltaic properties of low-bandgap (0.7–0.9 eV) lattice-matched GaInNAsSb solar junctions grown by molecular beam epitaxy on GaAs. *Solar Energy Materials and Solar Cells*. 2019;195:198-203.

11. Ledentsov NN, Shchukin VA, Lyytikäinen J, et al. Green (In,Ga,Al)P-GaP light-emitting diodes grown on high-index GaAs surfaces. *Appl Phys Lett*. 2014;105:1-5. <https://doi.org/10.1063/1.4900938>
12. Aho A, Korpijärvi V-M, Isoaho R, et al. Determination of composition and energy gaps of GaInNAsSb layers grown by MBE. *J Cryst Growth*. 2016;438:49-54.
13. Espinet-González P, Rey-Stolle I, Ochoa M, Algora C, García I, Barrigón E. Analysis of perimeter recombination in the subcells of GaInP/GaAs/Ge triple-junction solar cells. *Prog Photovolt Res Appl*. 2015;23(7):874-882.
14. Perl EE, Simon J, Geisz JF, et al. Development of high-bandgap AlGaInP solar cells grown by organometallic vapor-phase epitaxy. *IEEE Journal of Photovoltaics*. 2016;6(3):770-776.
15. Faucher J, Sun Y, Jung D, Martin D, Masuda T, Lee ML. High-efficiency AlGaInP solar cells grown by molecular beam epitaxy. *Appl Phys Lett*. 2016;109(17):1-4.
16. Tukiainen A, Likonen J, Toikkanen L, Leinonen T. Unintentional boron contamination of MBE-grown GaInP/AlGaInP quantum wells. *J Cryst Growth*. 2015;425:60-63.
17. Siefer G, Baur C, Bett AW. External quantum efficiency measurements of Germanium bottom subcells: measurement artifacts and correction procedures, 35th IEEE Photovoltaic Specialists Conference, 2010. pp. 000704-000707.

How to cite this article: Aho A, Isoaho R, Raappana M, et al. Wide spectral coverage (0.7–2.2 eV) lattice-matched multijunction solar cells based on AlGaInP, AlGaAs and GaInNAsSb materials. *Prog Photovolt Res Appl*. 2021;29: 869–875. <https://doi.org/10.1002/pip.3412>